Research Square

Preprints are preliminary reports that have not undergone peer review.
They should not be considered conclusive, used to inform clinical practice,
or referenced by the media as validated information.

Antineoplastic Efectiveness of Silver Nanoparticles Synthesized from *Onopordum Acanthium* L. extract (AgNPs-OAL) toward MDA-MB231 Breast Cancer Cells

Romina Delalat
Department of Biology, Central Tehran Branch, Islamic Azad University, Tehran, Iran
Seyed Ataollah Sadat Shandiz (atashandiz@yahoo.com)
Islamic Azad University of Tehran: Islamic Azad University Central Tehran Branch
Bahareh Pakpour
Department of Biology, Central Tehran Branch, Islamic Azad University, Tehran, Iran

Research Article

Keywords: silver nanoparticles, anticancer, reactive oxygen species, Apoptosis.

Posted Date: July 27th, 2021

DOI: https://doi.org/10.21203/rs.3.rs-730515/v1

License: This work is licensed under a Creative Commons Attribution 4.0 International License.
Read Full License

Abstract

The present research was done to investigate the anticancer properties of silver nanoparticles (AgNPs) fabricated using bioactive extract of *Onopordum acanthium* L. (AgNPs-OAL) against breast cancer cell MDA_MB231 *in vitro*. The determination studies of AgNPs-OAL were confirmed by X-ray diffraction (XRD), field emission scanning electron microscopy (FESEM) analysis. Interestingly, FESEM image observed the spherical shape of AgNPs-OAL with the range of 1–100 nm. As AgNP-OAL exhibited significant cytotoxicity properties on breast cancer MDA_MB231 cells with IC_{50} values of 66.04 µg/mL, while lowing toxicity toward normal human embryonic kidney 293 (HEK293) cells with IC_{50} values of 101.04 µg/mL was evaluated. Further, up-regulation of apoptotic *Bax* and *CAD* genes expressions were confirmed by quantitative real-time reverse transcription-PCR (qRT-PCR) technique results. Moreover, enhanced cell cycle population (sub-G1), annexin V/PI staining, acridine orange and ethidium bromide (AO/EB) staining, Hoescht 33258 dye, and generation of reactive oxygen species (ROS) observed in AgNP-OAL-treated MDA_MB231 cancer cells. The green-synthesized AgNP-OAL has promising anticancer efficiency that can trigger apoptosis pathway in the MDA_MB231 breast cancer cells.

Introduction

According to the global cancer burden based on the GLOBOCAN 2020, it was estimated that 19.3 million new cancer cases and almost 10.0 million cancer deaths happened in 2020. Breast cancer is the most frequently diagnosed cancer, with almost 2.3 million new cases reported to be distinguished in 2020 [1]. A large number of drugs in chemotherapy suffer from different side effects such as enhancing multi-drug resistance (MDR), poor solubility, and undesirable damage to normal cells, which indicates as results of commonly therapeutic intervention strategies [2].

Recently, the development of metal nanoparticles is gaining consideration, due to their cancer diagnosis, tumor imaging, and drug delivery [3]. Newly, silver nanoparticles (AgNPs) have been reported to display wound healing, antibacterial activities, [4] antimicrobial, [5] antioxidant, [6] and anticancer properties [7]. Fabrication of nanoparticles is mediated through a variety of chemical, physical, and biological strategies [8]. There is an increased interest in synthesis of nanoparticles by using green fabrication method using plants owning to their various advantages such as simple, cost effective, an environmentally eco-friendly, and do not require hazardous chemicals [9]. On the other hand, *Onopordum acanthium* L. is a flowering plant belonging to the family Asteraceae, with rich phytochemical compounds. *Onopordum acanthium* L. displayed significant medical activities such as antiradical, antibacterial, antihypertensive, cardiotonic agent, antitumor, and anti-inflammatory activities [10].

In this context, we have explored the apoptotic activity of AgNPs using *Onopordum acanthium* L. (AgNPs-OAL) extract as reducing agent. Field emission scanning electron microscopy (FESEM) was utilized to identify the morphological feature of the nanoparticles. Crystalline nature of nanoparticles was explored using XRD, and the *in vitro* cytotoxicity was performed in MDA-MB231 (human breast cancer), and HEK293 (human embryonic kidney) cell lines upon treatment with prepared AgNPs-OAL. Moreover, cell

cycle analysis, morphological properties of apoptotic/necrotic cells, ROS generation, apoptotic *Bax* and *CAD* gene expressions, and induction of apoptosis/necrosis were also evaluated by Annexin V/PI staining to explore the significant impacts of the AgNPs-OAL as anticancer agents.

Materials And Methods

Fabrication and determination of green AgNPs-OAL

For preparation of plant extract, the powder form (50 grams) of dried plant *Onopordum acanthium* L. was added to 200 cc of solvent ethanol (50%), and centrifuged for 20 min at 14000 rpm. The resulting extract was filtered through a filter paper, and then stored in the refrigerator prior to use. The extract of *Onopordum acanthium* L. about 5 mL was added dropwise in 100 mL 1 mM silver nitrate ($AgNO_3$, 99%) solution with constant stirring at room temperature. To collect the suspension, *Onopordum acanthium* L. extract-derived AgNPs (AgNPs-OAL) were centrifuged at 13000 rpm for 20 min. The determination studies were confirmed by X-ray diffraction (XRD), field emission scanning electron microscopy (FESEM) analysis. The crystalline nature of AgNPs-OAL was characterized by XRD (Burker AXS D8 X-Ray diffractometer) instrument using Cu Kα radiation in 2θ range of 5°–80°. The particle morphology of prepared AgNPs-OAL was imaged and analyzed through FESEM (Philips XL30) instrument.

Cell culture

MDA-MB231 (human breast cancer), HEK293 (human embryonic kidney) cell lines were procured from NCBI (National Cell Bank of Iran), Pasteur Institute of Iran. The cells were sustained in $RPMI_{1640}$ media pH = 7.2 with 10% FBS serum. The medium were added with 1% penicillin/streptomycin solution, followed by incubation at 5% CO2, 37°C.

Viability assay

The percentage of cell viability has been evaluated toward MDA-MB231 and HEK293 cell lines via MTT method followed by treatment with AgNPs-OAL according to previous standard protocol [11]. All the cells (1×10^4 cell /well) were grown in 96-well plates and exposed to various test doses (0, 0.625, 12.5, 25, 50, and 100 µg/mL) of AgNPs-OAL. After 24 hours incubation, MTT solution (5 mg/mL) was introduced into each well for 4 hours. The formazan crystals formed followed by adding MTT dye. To improve dissolving, DMSO solution was added to samples followed by recording the absorbance value at 570 nm using an ELISA microplate reader.

Analysis of apoptotic gene expressions

The apoptotic *Bax* and *CAD* gene expressions in AgNPs-OAL-treated cells were distinguished through SYBR Green real-time quantitative PCR at mRNA level. First, the cells were treated with AgNPs-OAL in IC_{50} concentration overnight. RNA-isolation kit was used for the isolation of the total cellular RNA (Qiagen, Valencia, CA) based on manufacturer's protocols. Then, complementary DNA (cDNA) was fabricated in terms of the manufacturer's protocols using a PrimeScript™ RT Kit (Takara, Japan). The primers utilized

for RT-PCR were: forward 5' CGGCAACTTCAACTGGGG 3' and reverse 5' TCCAGCCCAACAGCCG 3' for *Bax*, forward 5' TGGCAGAGATCGGAGAGCAT 3' and reverse 5' TCCTTCCATCCCTTCAGAGACTT 3' for *CAD*. Also, the sequence of the forward primer for Glyceraldehyde 3 phosphate Dehydrogenase *(GAPDH)* as a housekeeping gene was 5' CCCACTCCTCCACCTTTGAC 3' and that of reverse primer was 5' CATACCAGGAAATGAGCTTGACAA 3'. The ratio formula ($2^{-\Delta\Delta Ct}$) was used to assess the apoptotic gene expressions.

In vitro Apoptosis/necrosis assay

The quantification of the mode of AgNPs-OAL-induced cell death in the MDA-MB231 cells were assessed using flow cytometry followed by staining with fluorescein isothiocyanate (FITC)-Annexin V and propidium iodide (PI) staining in terms of the kit's Protocol (Roch, Switzerland). For this, the cells (3×10^5 cells/well) were subjected to 66.04 µg/mL of AgNPs-OAL, allowed to grow for 24 h. Washing of the treated cells was done by PBS, re-suspended in binding buffer, and staining with propidium iodide and Annexin V followed by incubation in the dark. After incubated for 10 min, the percentage of the apoptotic and necrotic cells was ascertained through flow cytometer.

2',7'-dichloro dihydro fluorescein diacetate (DCFH-DA) assay

Intracellular ROS generation was distinguished using flow cytometry. The cells (MDA-MB231, 3×10^5 cell /well) were seeded in 6-well plates for 24 h followed by the addition of required concentration of AgNPs-OAL. The MDA-MB231 cells were washed with phosphate-buffered saline and then cells were exposed with DCFH-DA dye after a further treatment of 30 min. The stained cells were further investigated via flow cytometer for determination of ROS production.

Cell cycle analysis

To investigate the changes in cell cycle evaluation in AgNPs-OAL treated MDA-MB231 cells, flow cytometric analysis were determined. The MDA-MB231 cells were cultured in 6-well plates and exposed with 66.04 µg/mL of the AgNPs-OAL in the CO_2 incubator for 24h.

Further, the cells were harvested, and washed with PBS. After fixation in cold ice 70% ethanol, the cells were then stained with propidium iodide, followed by treatment of RNase A (100 µg/ml). Finally, the DNA content of stained cells was measured through flow cytometer.

Morphology of apoptotic/necrotic cells

Determination of apoptotic/necrotic cells was investigated by a dual acridine orange and ethidium bromide (AO/EB) and Hoechst nuclear staining. The MDA-MB231 cells were treated with 66.04 µg/mL of AgNPs-OAL. After washing with PBS, control and treated cells were fixed by 4% formaldehyde and stained with 10 µL of AO/EB solution for 5 min incubation.

For the Hoechst 33258 staining, MDA-MB231 cells were subjected to six-well plating, overnight incubation with AgNPs-OAL, staining with Hoechst 33258 solutions for 5 min in the dark, followed by washing thrice with PBS. For observation, treated and control cells were visualized for their apoptotic to nuclei using fluorescence microscopy image.

Result And Discussion

Characterization of AgNPs-OAL

In recent decades, silver nanoparticle fabricated using biological methods show promising impact toward cancer cell lines. Plant mediated green strategy for AgNPs synthesis can be superior to fungal and bacterial- mediated strategies because of their accessibility, environment friendly procedures and safety [12–14]. In this investigation, *Onopordum acanthium* L. extract was used for the fabrication of AgNPs. As the *Onopordum acanthium* L. extract was mixed with silver nitrate solution, the variation in color was seen in the solution that converted into the dark brown overnight, indicating the fabrication of silver nanoparticles by phytoconstituents of *Onopordum acanthium* L. extract.

XRD pattern of particles confirm the crystallinity level of the AgNPs-OAL' structure (Fig. 1). Intense peaks of silver nanoparticles from the extract of *Onopordum acanthium* L. were visualized at 37.93°, 43.88°, 64.13° and 77.13° in the 2θ range noted at (111), (200), (220) and (311) diffraction pattern, respectively. The reflection planes of the fabricated AgNPs-OAL were consistent with earlier investigations [15, 16]. In order to find out the shapes and morphology of the produced AgNPs-OAL, the field emission scanning electron microscopy (FESEM) analysis was investigated. The AgNPs-OAL was spherically shaped with a size in the range of 1–100 nm (Fig. 2).

Cytotoxicity effect of AgNPs-OAL on MDA-MB-231cells

In the current investigation, cytotoxicity of AgNPs-OAL was examined toward human breast cancer (MDA-MB-231) human embryonic kidney (HEK293) cells at concentration of 6.25 to 100 µg/mL using MTT assay. Interestingly, AgNPs-OAL has exhibit significant dose-dependency on cell viability followed by increasing concentrations. The IC_{50} values of AgNPs-OAL against MDA-MB231 and HEK293 cells were 66.04 and 101.04 µg/mL, respectively. The *in vitro* cell viability was exhibited as 85% in AgNPs-OAL at 12.5 µg/mL however; the percentage of viability was remarkably reduced as 45% at 100 µg/mL of nanoparticles (Fig. 3). Herein, we showed that MDA-MB-231 cells are more sensitive to AgNPs-OAL than normal HEK293 cells. Our results are in agreement with that of Gurunathan et al. (2013), where biologically synthesized AgNPs using culture supernatant of *Bacillus funiculus* recorded significant cytotoxicity against MDA-MB-231 cell line in a dose dependent manner, with IC_{50} value of 8.7 µg/mL [17]. Also, Ghandehari et al. (2019) reported apoptotic properties of *Rubia tinctorum* produced AgNPs toward MDA-MB-231 cell line (IC_{50} = 4 µg/mL/48 h). These finding imply that fabricated AgNPs-OAL depressed MDA-MB-231 cell viability [18]. According to our MTT results, AgNPs-OAL exhibited dose–dependent relationship on the viability of MDA-MB-231cells, which could be relevant to the synergetic activities of

functional groups origin from *Onopordum acanthium* L. attaching to the AgNPs. Moreover, the impacts of green-fabricated AgNPs in MDA-MB-231 are consistent with earlier studies [19, 20].

Measurement Of Reactive Oxygen Species Production

Reactive oxygen species (ROS) produced in normal cells and have roles in many physiological conditions [21]. Under excessiveness of ROS, a series of cellular events were occurring results in lipid peroxidation, DNA damaging, cell cycle arrest, and promote apoptosis pathway [22]. It has been reported that new strategies for targeting ROS contribute to the cancer therapy [23]. Various reports have elucidated the roles of different nanometals in triggering ROS content in different cancer cells [24, 25]. Zhu et al. reported that AgNPs can induce human hepatocellular carcinoma HepG-2 cell apoptosis via ROS-mediated MAPKs, AKT, and p53 signaling pathways [26]. Moreover, ROS production in cancers modulates the different signaling pathways by regulating apoptosis, angiogenesis and proliferation [27].

In our study, ROS production in treated MDA-MB231 cells was 71.7%, while the control cells were 4.08%. In the current work, the ROS production in MDA-MB231 cells was illustrated in Fig. 4. Maximum production of ROS was closely exhibited for AgNPs-OAL, resulting in high cytotoxicity on MDA-MB231 cells as presented in the above results.

Agnps-oal Induce Apoptosis In Mda-mb231 Cells

Apoptosis represents a well defined intracellular physiological cell death with often doesn't trigger inflammatory response [28]. Effector caspase 3 activation is required for efficient execution of apoptotic death [29]. Translocation and cleavage of caspase-activated DNAse (CAD) were activated by caspase 3, results in DNA fragmentation.

In the current study, we evaluated the roles of pro-apoptotic *Bax* and *CAD* regulation in relation to the apoptotic death of cancer cells [22]. The mRNA expression levels of genes in AgNPs-OAL - mediated apoptotic cells were displayed by qRT-PCR method, which is presented in Fig. 5. The expression of the *CAD* and pro-apoptotic *Bax* genes was found to enhance by a 4.04-fold and 1.38 fold in AgNPs-OAL treated MDA-MB231 cells, respectively.

The MDA-MB231 cells undergoing programmed cell death and necrosis were determined by the Annexin V/PI staining (Fig. 6). We found that the AgNPs-OAL enhanced the number of early and late apoptosis on MDA-MB231 by 47.8 % at 66.04 µg/mL. In the report conducted by Mohammadi-Ziveh et al., the apoptotic properties of Ag-*S.Khuzistanica* on the colorectal HT29 cancer cell line were investigated. They indicated that 375, 750, 1500, 3000 µg/mL of Ag- *S.Khuzistanica* can increase the apoptosis rate (~ 30%) along with the up-regulation of apoptotic index ratio. In our study, the apoptosis rate (47.8 %) was much higher after exposing to AgNPs-OAL as compared with the Mohammadi-Ziveh results (~ 30%) [30].

Considering the main pattern of nanoparticles in the apoptosis, the cell cycle results were conducted in the AgNPs-OAL -exposed MDA-MB231 cells. The cellular DNA of treated MDA-MB231 cells was stained with PI followed by testing the DNA content via flow cytometry assay. Herein, the proportion of AgNPs-OAL-exposed cells in the apoptotic cell population (sub-G1) phase was increased from 7.04–12.58% in MDA-MB231 cells (Fig. 7). A comparison of the Annexin V/PI staining and cell cycle results indicates that the exposure of MDA-MB231 cells with AgNPs-OAL cause to inhibition of sub-G1 phase and the up-regulation of apoptosis by increasing early and late phase of apoptosis pathway.

Moreover, we employed a further examination to determine the possible stimulation role of AgNPs-OAL in apoptosis pathway. Given that the previous section demonstrated that the AgNPs-OAL has the capability of triggering an apoptosis pathway, the alterations in the nuclear morphology of apoptotic, necrotic cells was tested by AO/EB double staining and Hoescht 33258 after treated with AgNPs-OAL.

The Hoescht 33258 results display that AgNPs-OAL-treated cells has enhanced apoptosis via cell structure abnormality, bright color, and condensed chromatin (Fig. 8).

At concentration of 66.04 µg/mL, AO/EB double staining was investigated to discriminate the variations in apoptotic and normal cells. The Fig. 9 shows that treated cells display apoptosis by changing color of the nucleus into orange, while green nuclei represent untreated cells. Nanoparticles-exposed MDA-MB231 cells demonstrated an increase in the cell shrinkage and nuclear fragmentation as compared to untreated cells, exhibiting the promotion of apoptosis pathway by the fabricated AgNPs-OAL. Thus, the results exhibited that the AgNPs-OAL increased cell death, leading to the induction of apoptosis pathway.

Conclusion

In summary, plant-mediated AgNPs synthesis from *Onopordum acanthium* L. extract was generated by green fabrication route. Determinations of the obtained nanoparticles were conducted by FESEM and XRD analysis. The results of *in vitro* cytotoxicity assay, apoptotic genes expressions, cell cycle analysis, annexin V/PI staining, AO/EB staining, Hoescht 33258 staining, and generation of reactive oxygen species (ROS) exhibited that fabricated AgNPs could act as a promising strategy in treating breast cancer in future.

Declarations

Conflict of interest

The authors declare no conflict of interest.

Author contributions

Conceptualization: SASS and RD, Methodology: SASS, Formal analysis: RD, Investigation: RD, Resources: AS, Data curation: SASS and BP, Writing—original draft preparation: SASS, Visualization: SASS and BP supervision, SASS.

References

1. Sung H, Ferlay J, Siegel R L, Laversanne M, Soerjomataram I, Jemal A, Bray F. (2021) Global cancer statistics 2020: GLOBOCAN estimates of incidence and mortality worldwide for 36 cancers in 185 countries. CA:A Cancer J Clininc 71(3):209-249.
2. Acharya D, Satapathy S, Somu P, Kumar Parida U, Mishra G (2020) Apoptotic Effect and Anticancer Activity of Biosynthesized Silver Nanoparticles from Marine Algae Chaetomorpha linum Extract Against Human Colon Cancer Cell HCT-116. Biol Trace Elem Res 199(5): 1812-1822.
3. Kumari R, Saini AK, Kumar A, Saini RV (2019) Apoptosis induction in lung and prostate cancer cells through silver nanoparticles synthesized from *Pinus roxburghii* bioactive fraction. JBIC J Biol Inorg Chem 25: 23-37.
4. Riaz M, Mutreja V, Sareen S. et al (2021) Exceptional antibacterial and cytotoxic potency of monodisperse greener AgNPs prepared under optimized pH and temperature. Sci Rep 11: 2866. https://doi.org/10.1038/s41598-021-82555-z
5. Soliman H, Elsayed A, Dyaa A (2018) Antimicrobial activity of silver nanoparticles biosynthesised by Rhodotorula sp. strain ATL72, Egyptian J Basic Appl Sci5 (3): 228-233.
6. Salari S, Esmaeilzadeh Bahabadi S, Samzadeh-Kermani A, Yosefzaei F (2019) *In-vitro* Evaluation of Antioxidant and Antibacterial Potential of Green Synthesized Silver Nanoparticles Using *Prosopis farcta* Fruit Extract, Iran J Pharm Res 18(1): 430–455.
7. Venugopal K, ARather H, Rajagopal K, Shanthi M P, Sheriff K, Illiyas M,et al (2017) Synthesis of silver nanoparticles (Ag NPs) for anticancer activities (MCF 7 breast and A549 lung cell lines) of the crude extract of *Syzygium aromaticum*. J Photochem Photobiol B Biol 167: 282-289.
8. Almalki MA, Khalifa AYZ (2020) Silver nanoparticles synthesis from Bacillus sp KFU36 and its anticancer effect in breast cancer MCF-7 cells via induction of apoptotic mechanism. J Photochem Photobiol B Biol 204: 111786.
9. Kiran P. Shejawal, Dheeraj S. Randive, Somnath D. Bhinge, Mangesh A. Bhutkar, Sachin S. Todkar, Anjum S. Mulla, Namdeo R. Jadhav (2021) Green synthesis of silver, iron and gold nanoparticles of lycopene extracted from tomato: their characterization and cytotoxicity against COLO320DM, HT29 and Hella cell. J Mat Sci: Mat Med 32,19: https://doi.org/10.1007/s10856-021-06489-8.
10. Garsiya ER, Konovalov DA, Shamilov AA, Glushko MP, Orynbasarova KK (2019) A Traditional Medicine Plant, *Onopordum acanthium* L. (Asteraceae): Chemical Composition and Pharmacol Research. Plants (Basel) 8(2):40.
11. Hira I, Kumar A, Kumari R, Saini AK, Saini RV (2018) Pectinguar gum-zinc oxide nanocomposite enhances human lymphocytes cytotoxicity towards lung and breast carcinomas. Mater Sci Eng C 90:

494–503.

12. Ratan ZA, Haidere MF, Nurunnabi M, Shahriar SM, Ahammad A, Shim YY, et al (2020) Green Chemistry Synthesis of Silver Nanoparticles and Their Potential Anticancer Effects. Cancers 12(4): 855. https://doi.org/10.3390/cancers12040855.
13. Wang T, Yang L, Zhang B, Liu J (2010) Extracellular biosynthesis and transformation of selenium nanoparticles and application in H_2O_2 biosensor, Colloids Surf B Biointerfaces 80(1): 94–102.
14. Chen H, Yoo JB, Liu Y, Zhao G (2011) Green synthesis and characterization of se nanoparticles and nanorods. Electron Mater Lett 7: 333–336.
15. Prakash P, Gnanaprakasam P, Emmanuel R, Arokiyaraj S, and Saravanan M (2013) Green synthesis of silver nanoparticles from leaf extract of *Mimusops elengi*, Linn. for enhanced antibacterial activity against multi drug resistant clinical isolates, Colloids Surf B Biointerfaces 108: 255–259.
16. Das J, Das MP, Velusamy P (2013) *Sesbania grandiflora* leaf extract mediated green synthesis of antibacterial silver nanoparticles against selected human pathogens, Spectrochim Acta Part A 104: 265–270.
17. Gurunathan S, Woong Han J, Eppakayala V, Jeyaraj M, Kim JH (2013) Cytotoxicity of Biologically Synthesized Silver Nanoparticles in MDA-MB-231 Human Breast Cancer Cells. Biomed Res Int 2013; 2013: 535796. https://doi.org/10.1155/2013/535796.
18. Ghandehari S, Homayouni Tabrizi M, Ardalan P, Neamati A, Shali R (2019) Green synthesis of silver nanoparticles using Rubia tinctorum extract and evaluation the anti-cancer properties *in vitro*. IET Nanobiotechnol 13(3): 269-274.
19. Bandyopadhyay A, Roy B, Shaw P. et al (2020) Cytotoxic effect of green synthesized silver nanoparticles in MCF7 and MDA-MB-231 human breast cancer cells *in vitro*. Nucleus 63(2): 191–202.
20. Juarez-Moreno K, Gonzalez EB, Girón-Vazquez N, Chávez-Santoscoy RA, Mota-Morales JD, Perez-Mozqueda LL, et al (2017) Comparison of cytotoxicity and genotoxicity effects of silver nanoparticles on human cervix and breast cancer cell lines. Hum Exp Toxicol 36(9): 931-948.
21. Phaniendra A, Jestadi DB, Periyasamy L (2015) Free radicals: properties, sources, targets, and their implication in various diseases. Indian J Clin Biochem 30(1):11-26.
22. Ullah I, Talha Khalil A, Ali M, Iqbal J, Ali W, Alarifi S, et al (2020) Green-Synthesized Silver Nanoparticles Induced Apoptotic Cell Death in MCF-7 Breast Cancer Cells by Generating Reactive Oxygen Species and Activating Caspase 3 and 9 Enzyme Activities, Oxid Med Cell Longev 2020(4): 1215395. https://doi.org/10.1155/2020/1215395.
23. Mitra S, Nguyen LN, Akter M, Park G, Choi EH, Kaushik NK (2019) Impact of ROS generated by chemical, physical, and plasma techniques on cancer attenuation. Cancers 11(7):1030-1061.
24. Nourmohammadi E, Sarkarizi HK, Nedaeinia R, et al (2019) Evaluation of anticancer effects of cerium oxide nanoparticles on mouse fibrosarcoma cell line. J Cell Physiol 234(4): 4987-4996.

25. Khan BF, Hamidullah, Dwivedi S, Konwar R, Zubair S, and Owais M (2019) Potential of bacterial culture media in biofabrication of metal nanoparticles and the therapeutic potential of the as-synthesized nanoparticles in conjunction with artemisinin against MDA-MB-231 breast cancer cells. J Cell Physiol 234(5):6951-6964.
26. Zhu B, Li Y, Lin Z, et al (2016) Silver Nanoparticles Induce HePG-2 Cells Apoptosis through ROS-Mediated Signaling Pathways. Nanoscale Res Lett 11:198. doi:10.1186/s11671-016-1419-4
27. NavaneethaKrishnan S, Rosales JL, Lee KY (2019) ROS-mediated cancer cell killing through dietary phytochemicals. Oxid Med Cell Longev 2019: 9051542. doi: 10.1155/2019/9051542.
28. Rock KL, Kono H (2008) The inflammatory response to cell death. Annu Rev Pathol 3: 99-126. doi:10.1146/annurev.pathmechdis.3.121806.151456
29. Brentnall M, Rodriguez-Menocal L, De Guevara RL, et al. (2013) Caspase-9, caspase-3 and caspase-7 have distinct roles during intrinsic apoptosis. BMC Cell Biol 14:32. https://doi.org/10.1186/1471-2121-14-32
30. Mohammadi-Ziveh Z, Mirhosseini S A, Mahmoodzadeh Hosseini H (2020) *Satureja Khuzestanica* Mediated Synthesis of Silver Nanoparticles and Its Evaluation of Antineoplastic Activity to Combat Colorectal Cancer Cell Line. Iran J Pharm Res 19(4):169-180.

Figures

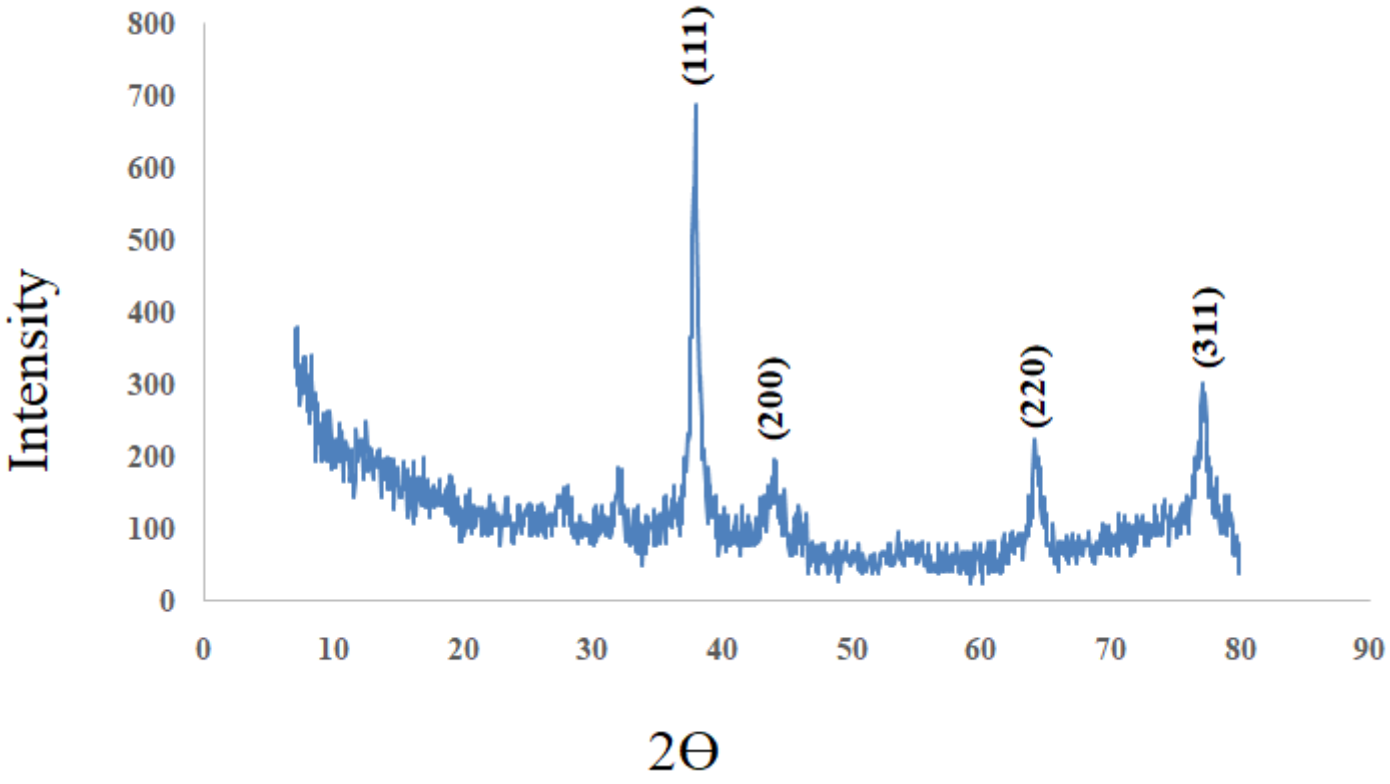

Figure 1

X-ray powder diffraction pattern of fabricated AgNPs-OAL.

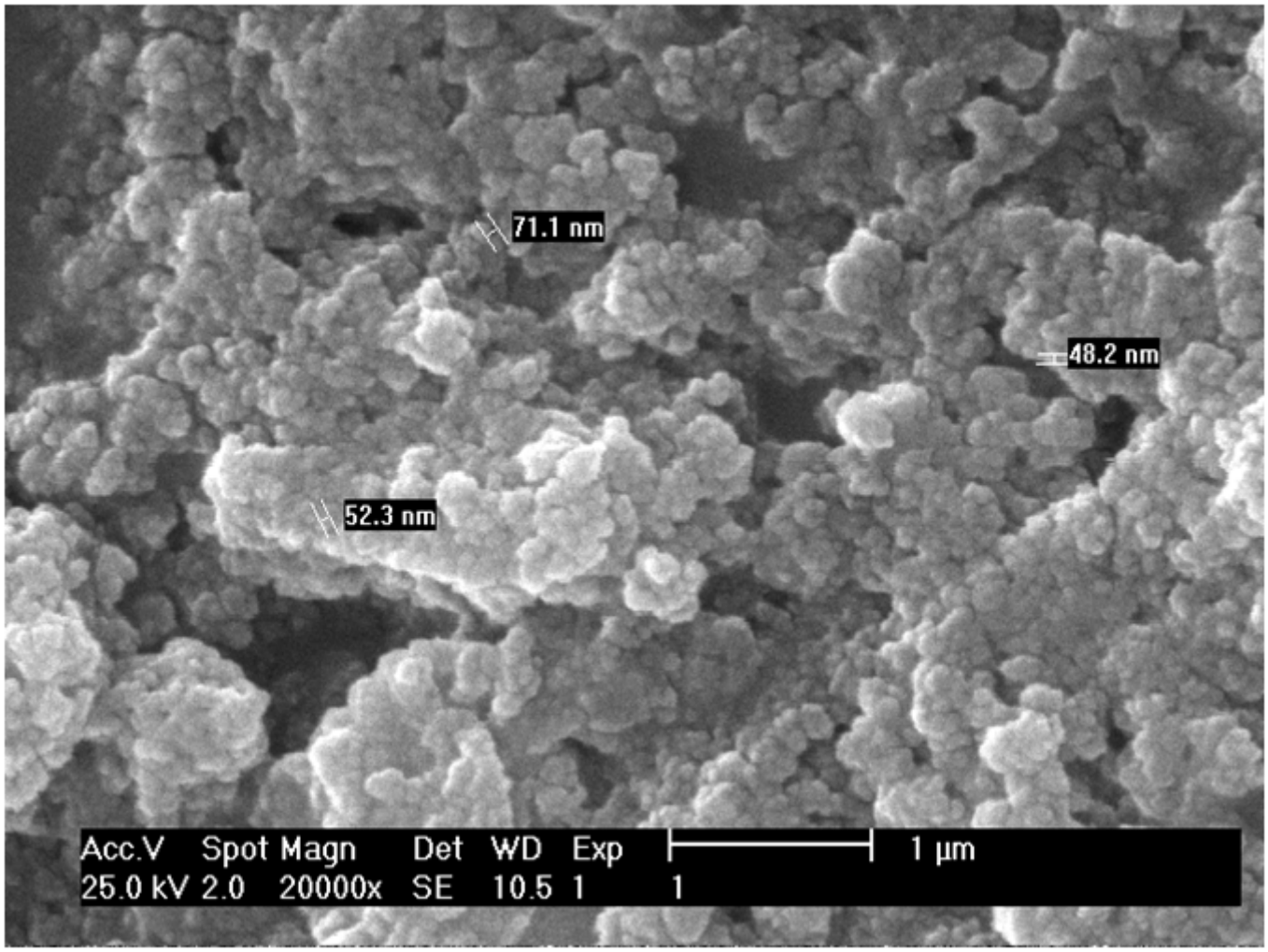

Figure 2

FESEM image of the silver nanoparticles fabricated using bioactive extract of Onopordum acanthium L

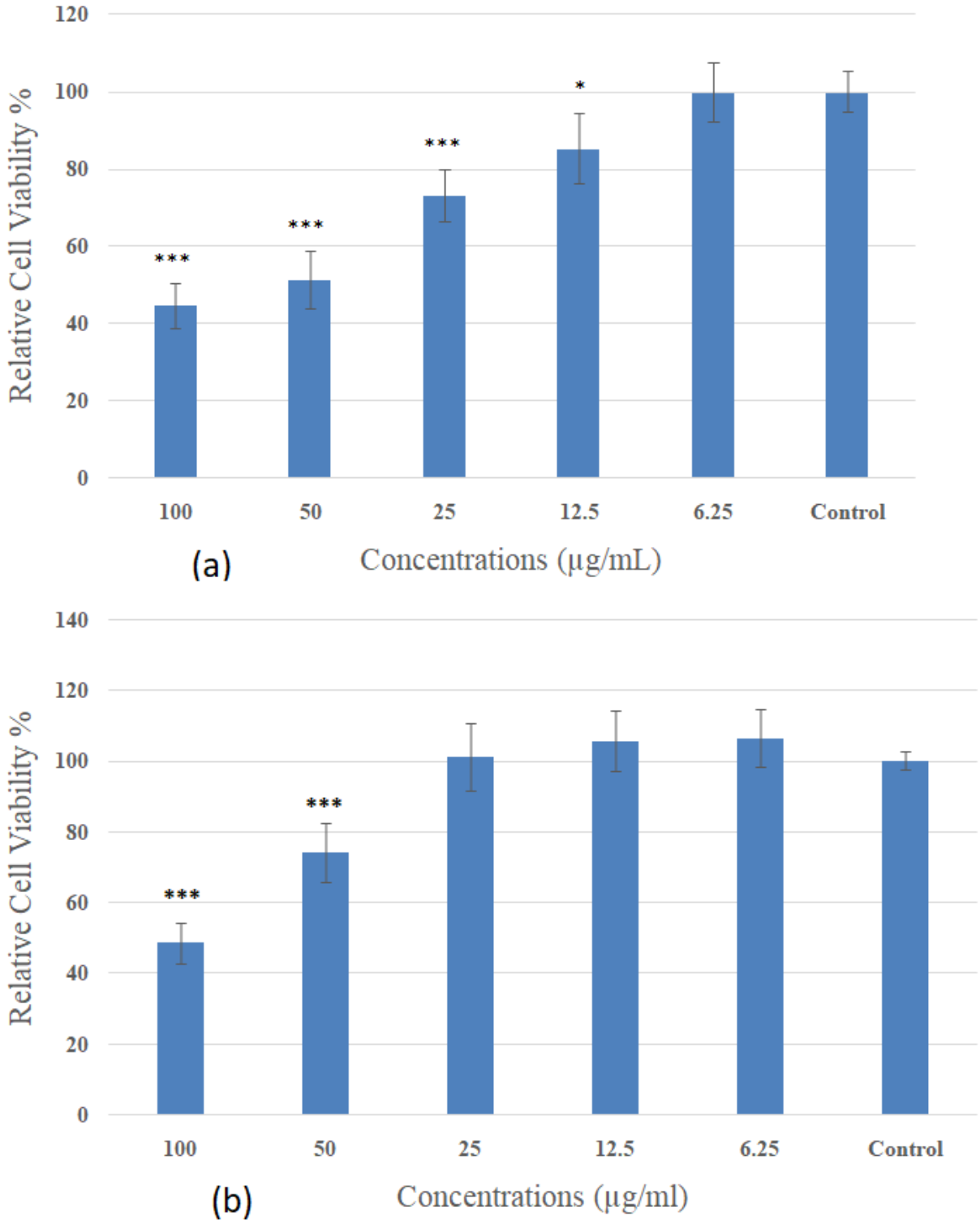

Figure 3

Percentage of (a) viable MDA-MB231 and (b) HEK293 cell lines exposed with AgNPs-OAL at different concentrations after overnight treatment. The data are presented as the mean ± SEM.

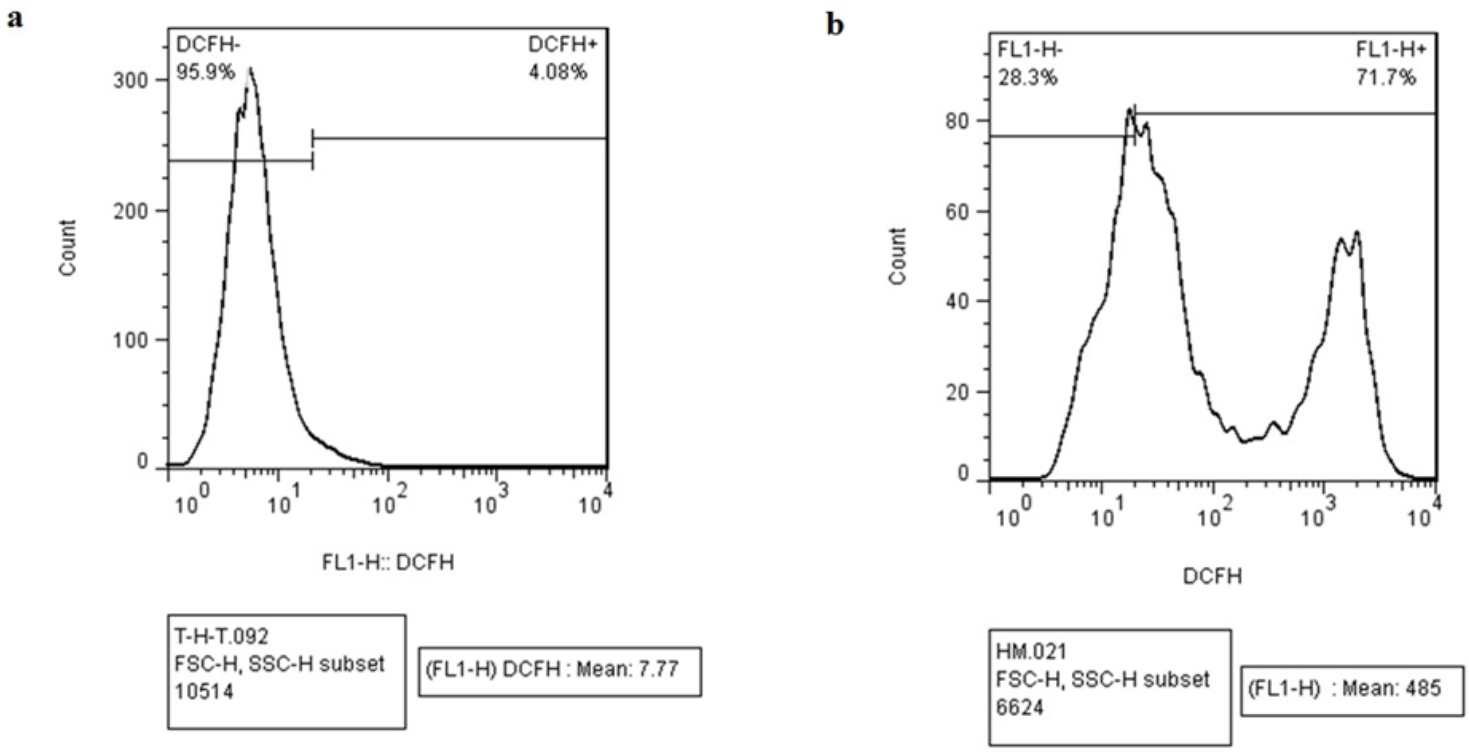

Figure 4

Effect of the produced AgNPs-OAL on ROS generation in untreated (a) and treated (b) MDA_MB231 cells utilizing DCFH-DA followed by flow cytometry.

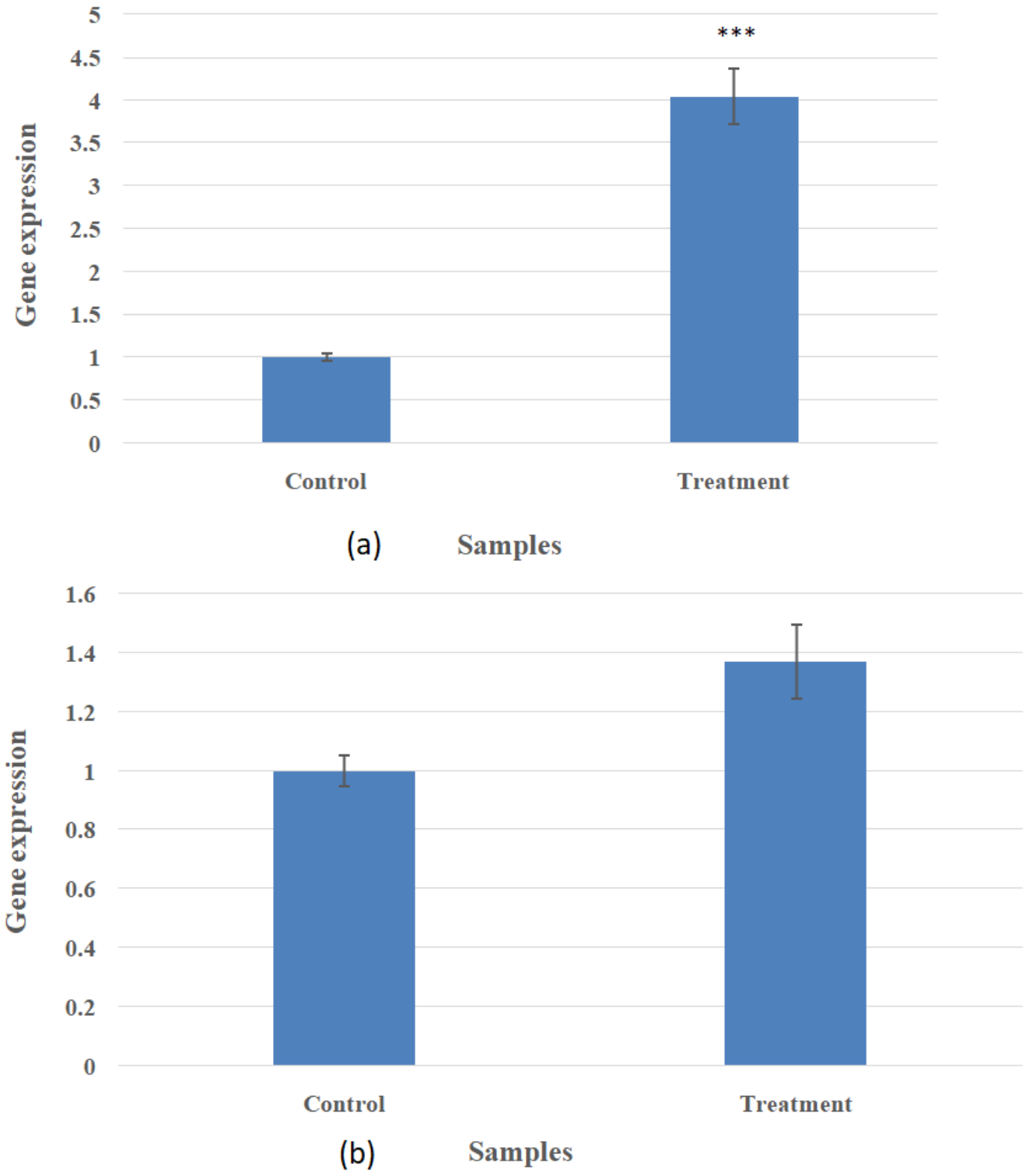

Figure 5

(a) Apoptotic CAD and (b) Bax genes expression analysis in MDA-MB231 cells with AgNPs-OAL compared with control.

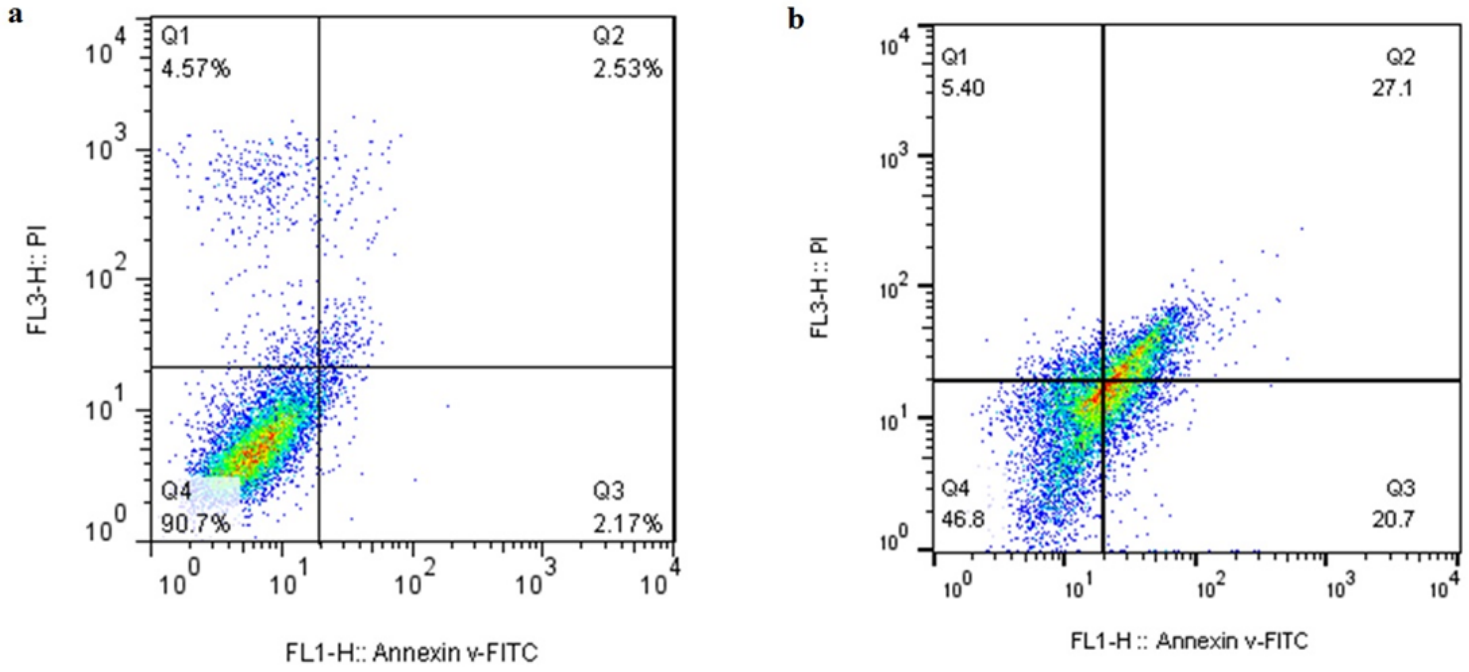

Figure 6

Evaluation of apoptosis/necrosis in MDA-MB231 cancer cells by flow cytometric analysis. (a) Negative control (b) Annexin/PI staining of exposed cells to AgNPs-OAL at 66.04 µg/mL.

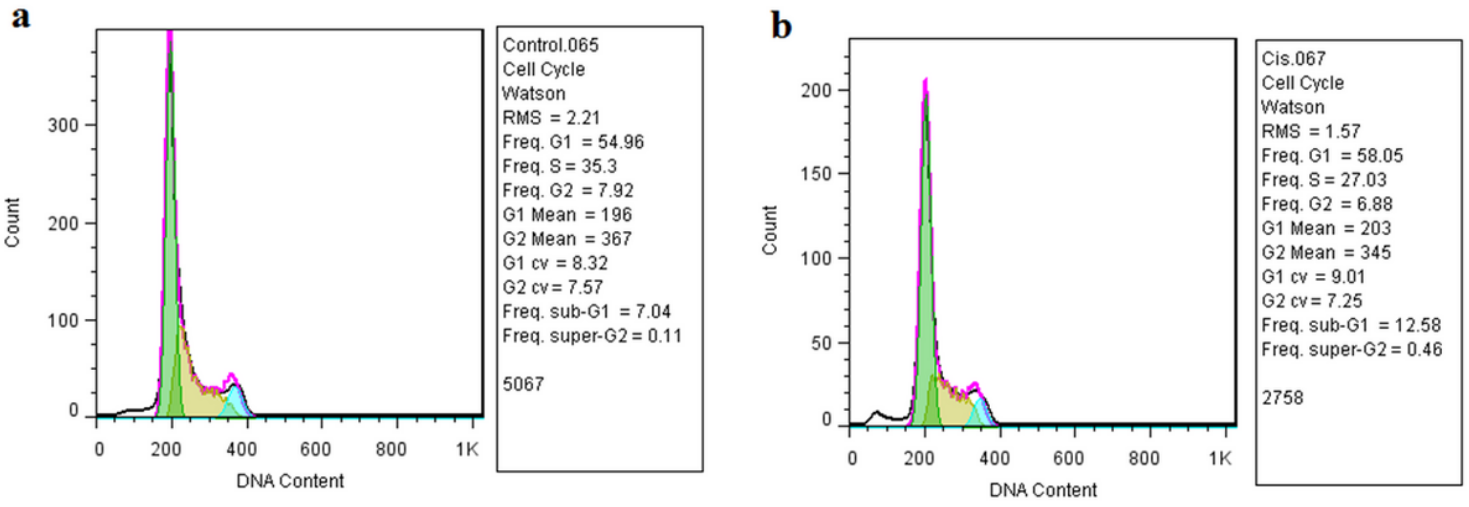

Figure 7

Effect of AgNPs-OAL after 24 h treatment on cell cycle arrest analysis of (a) untreated and (b) treated MDA-MB231 cells.

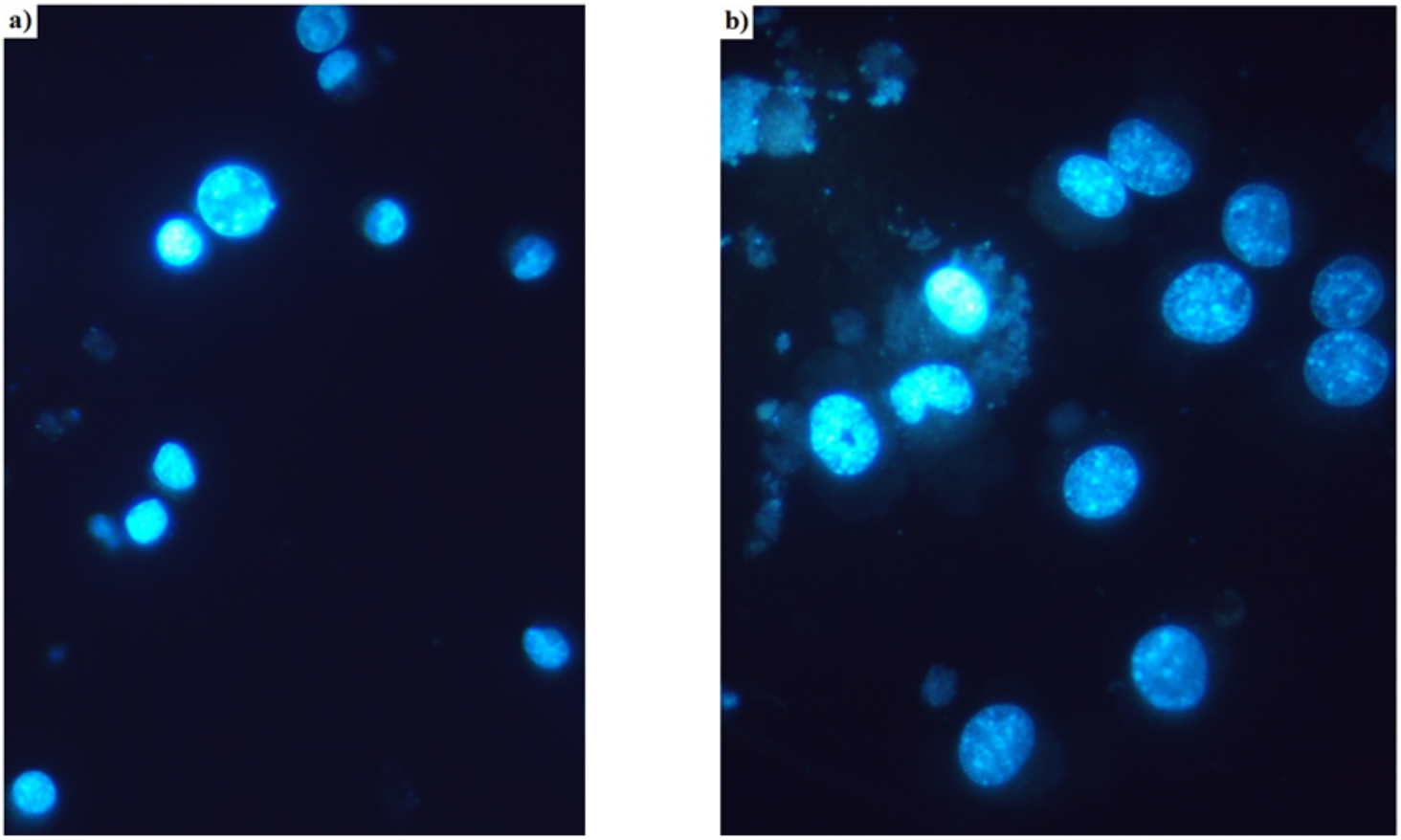

Figure 8

Morphology properties of MDA_MB231 cells with Hoescht 33258 staining under Fluorescence microscope, (a) untreatment as control (b) the cells exposed to IC50 of synthetic AgNPs-OAL for 24 hours.

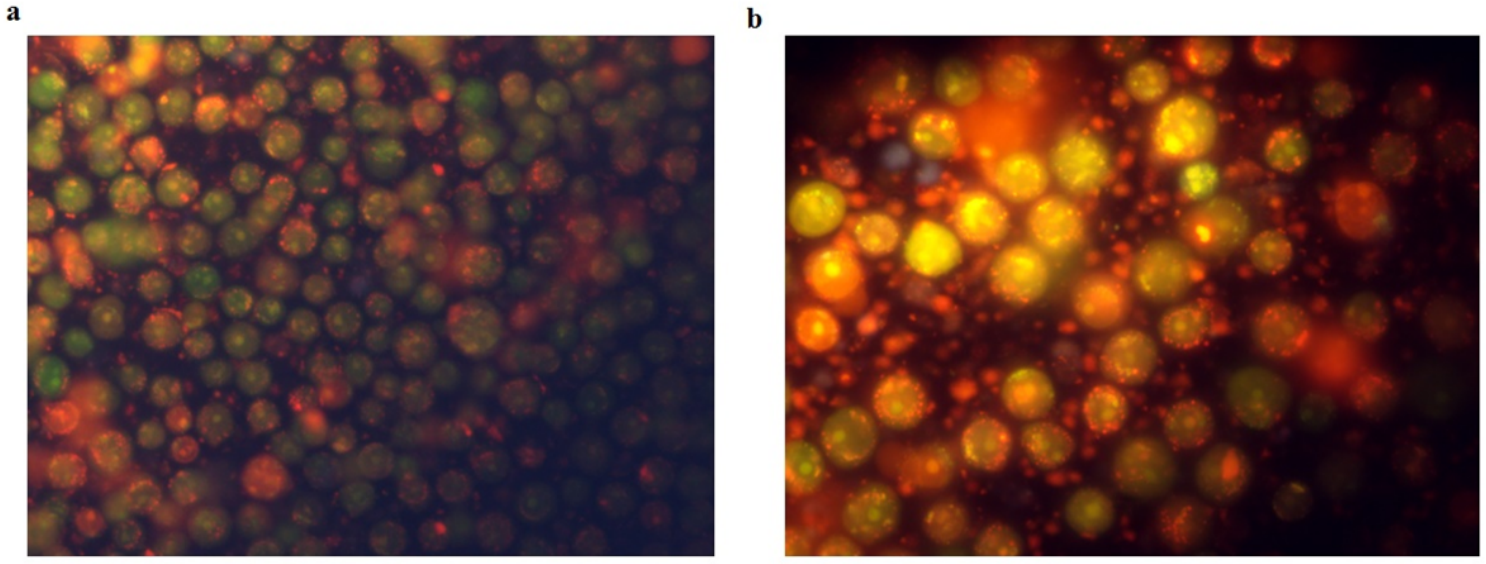

Figure 9

Morphology changes of (a) Untreated and (b) treated MDA_MB231 cells with fabricated AgNPs-OAL following AO/EB dye under Fluorescence microscope.